(2)

OFFICE OF NAVAL RESEARCH

CONTRACT NO. N0014-89-J-1746

R & T CODE 413r001

TECHNICAL REPORT NO. 14

Temperature Dependence of the Inverted Regime Electron Transfer Kinetics of Betaine-30 and the Role of Molecular Modes

Eva Åkesson, Alan E. Johnson, Gilbert C. Walker, Nancy E. Levinger, Thomas P. DuBruil and Paul F. Barbara

Journal of Chemical Physics, **96**, 7859 (1992)

University of Minnesota
Department of Chemistry
Minneapolis, MN 55455

May 18, 1992

69

J. Chem. Phys.

~~submitted~~

May 31, 1991

in press

Temperature Dependence of the Inverted Regime Electron Transfer Kinetics of Betaine–30 and the Role of Molecular Modes.

Eva Åkesson, Alan E. Johnson, Nancy E. Levinger, Gilbert C. Walker,

Thomas P. DuBruil[+], and Paul F. Barbara[*]

Department of Chemistry, University of Minnesota, Minneapolis, MN 55455

* Author to whom correspondence should be addressed

+ Deceased

Abstract

The inverted regime photoinduced electron transfer kinetics of betaine–30 have been investigated over a broad temperature range, revealing very little temperature dependence. For example, for betaine–30 in a polystyrene film, the electron transfer rate constant, k_{ET}, changes by less than a factor of 3 from T=293K to T=34K. The results are in striking contrast to predictions of contemporary electron transfer theories which employ classical nuclear modes to accept some or all of the energy of the electron transfer event. The comparison of theory and experiment for the betaines demonstrates that a full quantum mechanical theory is necessary to accurately describe the electron transfer kinetics of the betaines in environments with slow dielectric relaxation . The conclusions drawn for the betaines may also apply to other molecular examples of *inverted regime* electron transfer in slowly relaxing environments.

Contemporary electron transfer theory has had enormous success in accurately and quantitatively modeling a broad range of organic, inorganic, and biological electron transfer (ET) examples.[1] The foundation of ET theory involves a description of the ET event in terms of a localized electronic state of the electron donor Ψ_D and the localized state of the electron acceptor Ψ_A. The ET process is controlled by fluctuations of the nuclear coordinates of the solvent and solute. The various ET models differ in the way they treat the solvent and solute nuclear degrees of freedom, classically, quantum mechanically, or some combination thereof. Conventional models treat the solvent modes (the so–called solvent coordinate) classically, some assuming instantaneous equilibration of the solvent coordinate and others allowing for diffusive solvent coordinate motion.[2] For the vibrational modes of the reactants both quantum[5,6] and classical theories[4] have been formulated.[1,2] However, the quantum models that emphasize the high frequency vibrational modes still employ classical fluctuations of a *solvent and/or vibrational coordinate*[4] to accomplish the actual ET event.[5]

This paper is concerned with an experimental evaluation of the limitations of the classical aspects of ET theory. We investigate the temperature dependence of the ET rate constant k_{ET} for the photoinduced ET of betaine–30 as portrayed in Fig.1. This reaction[7-9] occurs in the Marcus inverted regime.[1] For theories which treat all modes classically, the reaction occurs near the crossing of the two electronic states, i.e. point *a* in Fig. 1. Mixed quantum/classical models[5,8] allow for multiple reaction regions, *b* points in Fig. 1., at each of the vibronic crossings 0→n, where n refers to the high frequency quantized vibrational levels of the product. The mixed quantal/classical models predict much lower activation energies and faster rates than the purely classical models for inverted regime ET. Recent experiments support the need for a quantum description of the vibrational modes of the reactant.[10,11]

The betaine class of compounds offers certain advantages for the study of quantum effects on ET kinetics. For instance, the betaines have extraordinarily large electronic coupling, V_{el}, which increases the magnitude of quantum effects on k_{ET}. Also, the various parameters necessary to apply ET theory, including the characteristic vibrational frequency ν, the vibrational (λ_{vib}) and solvent (λ_{solv}) reorganization energies, and V_{el}, can be directly evaluated by analyzing the charge transfer absorption band in Fig.1.[7,8] Finally, from an experimental perspective, the ET kinetics of betaine can be conveniently studied using ultrafast pump–probe spectroscopy.

Fig.2 portrays the transient pump–probe signal for betaine–30 in various environments. The pump pulse in each experiment induces a negative optical density change (upward direction in Fig.2) which recovers as the ET process occurs. Some of the transients also show evidence for relaxation of hot ground state molecules and a small component of photodecomposition which will be discussed in detail elsewhere.[12]

Two different spectrometers were used to record the transients in Fig.2. Both spectrometers employ an amplified 75–150fs near infrared dye laser.[13] One system uses a 8.2kHz copper vapor laser to pump the dye amplifier, while the other spectrometer uses a 500Hz Nd:YAG regenerative amplifier for the amplifier pump laser. Further experimental details are given in the figure captions and elsewhere.[12]

The contribution of the ET kinetics to the transients in Fig.2 is well modeled by a single exponential decay. The time constants from best–fits of the decay function to the data are interpreted as the inverse of the ET rate, k_{ET}. k_{ET} values for various solvents at a variety of temperatures are listed in Table 1. Table 2 lists k_{ET} as a function of temperature in polystyrene films. An Arrhenius plot for k_{ET} in the polar aprotic solvent triacetin is portrayed in Fig.3.

Some general conclusions can be drawn from these data and related experiments in

other solvents.[7] In polar solvents with $<\tau_s>$ larger than ≃ 5ps k_{ET} is faster than $<\tau_s>^{-1}$. $<\tau_s>$, the average solvation time, has been measured for many of these environments by the transient Stoke's shift method[2] and can be estimated in other cases from dielectric dispersion data[12] on the neat liquid using a continuum model.[2] For triacetin, $<\tau_s>^{-1}$ is listed as a function of temperature in Table 3. k_{ET} is orders of magnitude less sensitive to temperature than other examples of ultrafast intramolecular charge separation, such as the excited state ET of bianthryl.[14a] In fact, for betaine–30 in the non–polar polymer polystyrene, k_{ET} shows very little change from ambient temperature to 77°K (see Fig.4.) In a polystyrene film prepared by evaporation of a benzonitrile solution, the temperature dependence has been studied over an even larger temperature range and shows very little temperature dependence (see Fig.4) This latter film apparently includes a small amount of residual solvent, evidenced by an absorption maximum which is slightly offset toward the frequency of the absorption maximum of betaine in benzonitrile alone. The difference between the kinetics between films may reflect residual solvent.

Sumi and Marcus[4] recently formulated an ET theory that includes the effects of classical vibrational modes and classical solvent coordinate diffusion on k_{ET}. With the exception of $<\tau_s>$, all the required parameters for the Sumi/Marcus theory can be estimated from the spectral bandshape analysis of betaine–26 by Kjaer and Ulstrup.[8] (Betaine–26 and betaine–30 are similar molecules and should exhibit a similar dependence of the key parameters on the absorption maximum.) The procedure for extracting the various parameters will be given elsewhere.[7,12]

The Sumi/Marcus predictions are over 6 orders of magnitude slower than the observed rates (Fig.3) and exhibit a different temperature dependence than experiment. The small k_{ET} predicted by Sumi/Marcus theory is due to the classical requirement that the ET reaction occur at point *a* in Fig.1. The complex temperature dependence of k_{ET}

versus T^{-1} seen in Fig. 3. for the Sumi–Marcus theory reflects two effects: the temperature dependence of $<\tau_s>$ and the temperature dependence of $\bar{\nu}_{max}$, which causes a temperature dependence of ΔG^o, λ_{vib}, and λ_{solv}.

In contrast, the theory of Jortner and Bixon involves a sum of specific ET rates over individual vibronic channels

$$k^{0n}_{ET,JB} = k^{0n}_{NA}/(1+\mathscr{H}^{(n)}_A) \qquad (1)$$

where k^{0n}_{NA} is the nonadiabatic rate constant for the vibronic channel starting in vibrational level v=0 of DA and ending in v'=n of D^+A^-, see Fig. 1. $\mathscr{H}^{(n)}_A$ is the adiabaticity parameter for each channel. $\mathscr{H}^{(n)}_A$ and k^{0n}_{NA} are given by eqns 2 and 3 , respectively

$$\mathscr{H}^{(n)}_A = \frac{4\pi V^2_{el}}{\hbar \lambda_{solv,JB}} \frac{<\tau>_s}{} |<0|n>|^2 \qquad (2)$$

$$k^{0n}_{NA} = \frac{2\pi V^2_{el}}{\hbar (4\pi \lambda_{solv,JB} k_B T)^{\frac{1}{2}}} |<0|n>|^2 \exp\left[- \frac{(\Delta G^0_n + \lambda_{solv,JB})^2}{4\lambda_{solv,JB} k_B T} \right] \qquad (3)$$

Here $<0|n>$ is the Franck–Condon factor for the effective vibrational quantum mechanical mode included in the model and ΔG^o_n is the modified driving force for each vibronic channel, i.e.

$$\Delta G^o_n = \Delta G^o + nh\nu_{QM} \qquad (4)$$

The Jortner/Bixon model predicts a very different temperature dependence and a much faster rate than the Sumi/Marcus theory because the Jortner/Bixon approach allows for electron transfers in the *b* regions of Fig.1.

The predictions of the Jortner/Bixon model are also in strong disagreement with experiment in slowly relaxing solvents like triacetin[12]. The discrepancy can be traced to the classical treatment of the solvent coordinate. According to this approach, as $<\tau_S>$ increases the adiabicity parameter, $\mathscr{H}_A^{(n)}$, exceeds unity by orders of magnitude for the most favorable vibronic ET channels. For the sake of simplicity consider the 0→5 channel in Fig.1, which is nearly "barrierless", i.e. zero activation energy. If $\mathscr{H}_A^{(n)}$ is much greater than unity for this channel, then the channel will contribute $\simeq <\tau_s>^{-1}$ to the rate. Usually only one or perhaps two channels will contribute significantly because the activation energy of the other channels are much greater than zero. Consequently, if $<\tau_S>$ is very large and there exists a vibronic channel with nearly zero activation energy, the Jortner/Bixon theory predicts that k_{ET} will be roughly equal to $<\tau_s>^{-1}$ at the various temperatures.

The enormous discrepancy between the classical predictions of the Sumi/Marcus theory and the experimental observations dramatically demonstrate the importance of the high frequency vibrational modes in ET mechanisms. Other experimental observations supporting this conclusion have recently been reported.[10,11] Apparently, high lying channels, such as 0→5 in Fig.1, dominate the ET kinetics of betaine–30.

The Jortner/Bixon model predicts that k_{ET} for betaine–30 is on the order of $<\tau_S>^{-1}$; the rate is limited by the rate of fluctuations of solvent polarization. For quickly relaxing solvents, such as acetone, the experimentally measured k_{ET} is approximately equal to $<\tau_S>^{-1}$ in qualitative agreement with the Jortner/Bixon prediction.[7] However, in more slowly relaxing solvents $k_{ET} >> <\tau_S>^{-1}$. This is strong evidence that the so–called solvent coordinate is not the predominant accepting mode for the ET event in slowly relaxing environments. Rather the results suggest that that the solvent coordinate is *frozen* on the time scale of the ET event. The situation is complicated because all solvents, including triacetin, exhibit a distribution of relaxation times due to different solvation modes and

inertial effects.[2] However, the time scales and amplitudes of the various solvation components should be significantly temperature dependent, especially in the region of the glass transition (T≃ 268K) for triacetin. The absence of a strong temperature dependence for k_{ET} near the glass transition strongly rules out solvent fluctuations as the key element of the ET mechanism. The similarity of the rates in various nonpolar and polar, slowly relaxing solvents including nonviscous toluene, is evidence for a common ET mechanism. In these cases, the most likely mechanism involves *molecular modes* of betaine–30, itself. We envision the ET process to be in analogy with the fully quantum mechanical models for internal conversion of rigid, electronically excited molecules.[15] In addition to the high frequency mode that we have already included, there must be one or more low frequency, molecular modes which act as accepting modes for the energy during the ET event. The extremely mild temperature dependence for k_{ET} in polystyrene films indicate that a quantum mechanical description of the ET/internal conversion process is required to realistically model betaine–30. Work is in progress to identify the strongly coupled molecular modes for the ET process of betaine–30.

This research has been supported by the Office of Naval Research. E.Å. and N.E.L gratefully acknowledge postdoctoral fellowships from NFR (Swedish Natural Science Research Council) and the National Science Foundation, respectively. Helpful discussions with Profs. J.Jortner, S.Mukamel, and J.T.Hynes are gratefully acknowledged. This paper is dedicated to the memory of Thomas P. DuBruil.

1. G.L.Closs and J.R.Miller, Science **240**, 440 (1988); G.L.McLendon, Acc. Chem. Res. **21**, 160 (1988); R.A.Marcus and N.Sutin, Biochem. Phys. Acta **811**, 265 (1985); M.D.Newton and N.Sutin, Ann. Rev. Phys. Chem. **35**, 437 (1984).

2. For recent reviews and well referenced papers that discuss the role of solvation dynamics in ET see P.F. Barbara and W.Jarzeba, Adv. Photochem. **15**,1, 1990; M. Maroncelli, J. MacInnis and G.R. Fleming, Science **243**, 1674 (1989); J.D. Simon, *Acc. Chem. Res.*, **21**, 128 (1988); M.J. Weaver and G.E. McManis III, Acc. Chem. Res., **23**, 294 (1990).

3. J.T. Hynes, J. Phys. Chem. **90**, 3701 (1986).

4. H. Sumi and R.A. Marcus, J. Phys. Chem. **84**, 4894 (1986); W. Nadler and R.A. Marcus, J. Chem. Phys. **86**, 3906 (1987)

5. J. Jortner and M. Bixon, J. Chem. Phys. **88**, 167 (1988).

6. R.P.Van Duyne and R.S.Fisher, Chem. Phys. **5**, 183 (1974); V.G.Levich and R.R.Doganadze, Dokl. Akad. Nauk SSSR **133**, 158 (1960); N.R.Kestner, J.Logan, and J.Jortner, J. Phys. Chem. **78**, 2148 (1974); S.F.Fisher and R.P.Van Duyne Chem. Phys. **26**, 9 (1977); P.Siders and R.A.Marcus, J. Am. Chem. Soc. **103**, 748 (1981); R.A.Marcus, J. Chem. Phys. **81**, 4494 (1984).

7. E.Åkesson, G.C.Walker, and P.F.Barbara, J. Chem. Phys., ~~submitted~~ in press.

8. A.M. Kjaer and J. Ulstrup, J. Am. Chem. Soc. **109**, 1934 (1987).

9. (a) C. Reichardt, *Molecular Interactions*, vol 3, eds. H. Ratajczak and W.J. Orville–Thomas, John Wiley & Sons Ltd. (1982); (b) K. Dimroth, C. Reichardt, T. Siepmann and F. Bohlmann, Justus Liebigs Ann. Chem. **661**, 1 (1963); (c) C. Reichardt, Angew. Chem. Int. Ed. Engl. **18**, 98 (1979).

10. N.Liang, J.R.Miller, and G.L.Closs, J. Am. Chem. Soc. **112**, 5353 (1990).

11. I.R.Gould, R.H.Young, R.E.Moody, and S.Farid, J. Phys. Chem. **95**, 2068 (1991).

12 G.C.Walker, E.Åkesson, A.E.Johnson, N.E.Levinger, and P.F.Barbara, J. Phys. Chem., in preparation.

13. M.A. Kahlow, W. Jarzeba, T.P. DuBruil and P.F. Barbara, Rev. Sci. Instrum. **59**, 1098 (1988).

14. (a) T.J.Kang, W.Jarzeba, P.F.Barbara, and T.Fonseca, Chem. Phys. **149**, 81 (1990) (b) G.C.Walker, K.Tominaga and P.F.Barbara, unpublished C(t) results on GTA solvation measured using the linear wavelength with coumarin 153 at 293^{O}K. (c) V.Nagarajan, A.M.Brearley, T.J.Jang, and P.F.Barbara, J. Chem. Phys. **86**, 3183 (1987) (d) U.V.Khudayarov, and V.N.Khuderberdyev Russ. J. Phys. Chem. **64**, 1015, (1990). (e) A.M.Ras and P.Bordewijk, *Rec. Trav. Chim.* **90**, 1055 (1971). (f) E.Ikada and T.Watanabe, J. Phys. Chem. **78**, 1078 (1974).

15. P.Avouris, W.M.Gelbart, M.A.El–Sayed, Chem. Rev. **77**, 793 (1977).

Table 1. The Temperature Dependence of k_{ET}[a] of Betaine–30 in Various Solvents

Solvent	T(K)	$k_{ET}(10^{-12}sec^{-1})$	Solvent	T(K)	$k_{ET}(10^{-12}sec^{-1})$
triacetin			toluene		
	347	0.47 ± 0.06		331	0.55 ± 0.02
	333	0.43 ± 0.03		295	0.34 ± 0.02
	328	0.41 ± 0.02		293	0.31 ± 0.02
	323	0.40 ± 0.02		282	0.32 ± 0.04
	318	0.39 ± 0.02		269	0.29 ± 0.02
	314	0.34 ± 0.02		249	0.20 ± 0.01
	313	0.39 ± 0.04		223	0.15 ± 0.01
	308	0.36 ± 0.01			
	303	0.35 ± 0.04			
	295	0.29 ± 0.02	benzene		
	293	0.29 ± 0.01		331	0.50 ± 0.05
	271	0.22 ± 0.03		293	0.37 ± 0.03
	263	0.22 ± 0.02		286	0.42 ± 0.08
	259	0.26 ± 0.01		271	0.33 ± 0.07
	228	0.18 ± 0.02			

[a] The transient absorption data are fit to a functional form which is a sum of exponentials with (1) an extremely fast first component which for the purposes of this paper we treat as a coherent artifact and (2) a second component whose characteristic time we treat as the inverse of k_{ET}. In some polar solvents there is a third component with increased absorption ($+\Delta OD$) which may reflect hot ground state molecules and is discussed in reference 12.

Table 2. Electron Transfer Kinetics of Betaine–30 in Polystyrene.

Cast from benzonitrile solution[a]		Cast from methylene chloride solution[b]	
T(K)	$k_{ET}(10^{12}sec^{-1})$	T(K)	$k_{ET}(10^{12}sec^{-1})$
291	0.066 ± 0.003	293	0.11 ± 0.012
63	0.043 ± 0.004	144	0.091 ± 0.02
34	0.031 ± 0.004	76	0.077 ± 0.01

a An Arrhenius analysis yields the prefactor, $\log_{10}(A)=10.86$, and activation energy, $E_a=20cm^{-1}$.

b An Arrhenius analysis yields the prefactor, $\log_{10}(A)=11.09$, and activation energy, $E_a=27cm^{-1}$.

Table 3. Solvation Rates[a] and Theoretically Calculated[b] k_{ET} for Betaine–30 in Triacetin at Various Temperatures.

T K	$\langle\tau_s\rangle^{-1}$ $(10^{12}sec^{-1})$	$k_{ET,SM}$ $(10^{12}sec^{-1})$	$k_{ET,JB}$ $(10^{12}sec^{-1})$
318	0.1 – 0.07	$3x10^{-11} - 2x10^{-11}$	$3.0x10^{-2} - 2.1x10^{-2}$
313	0.06 – 0.05	$5x10^{-11} - 4x10^{-11}$	$3.0x10^{-2} - 2.5x10^{-2}$
308	0.04 – 0.03	$2x10^{-10} - 1x10^{-10}$	$2.4x10^{-2} - 1.8x10^{-2}$
303	0.03 – 0.02	$4x10^{-10} - 2x10^{-10}$	$2.8x10^{-2} - 1.7x10^{-2}$
293	0.02 – 0.01	$7x10^{-9} - 2x10^{-9}$	$1.6x10^{-2} - 4.0x10^{-3}$
283	$10^{-2} - 10^{-3}$	$1x10^{-7} - 1x10^{-8}$	$8.9x10^{-3} - 1.2x10^{-3}$
228[c]	$2x10^{-7} - 10^{-7}$	$5x10^{-8} - 2x10^{-13}$	$3.3x10^{-7} - 1.1x10^{-7}$

[a] Average solvation times, $\langle\tau_s\rangle$, were estimated various ways. The limits of the reported ranges each correspond to single exponential solvent relaxation times. The values at 228K are values of τ_l, the longitudinal relaxation time, estimated from the dielectric data found in refs. 14a (lower limit) and 14b (upper limit). The range of values at 283K derive from refs. 14c (lower limit), as estimated by time dependent Stokes shift measurements, and 14d (upper limit) as estimated by τ_l. The range at 293K derive from ref. 14e (lower limit) measured by single–wavelength method, time dependent – Stokes shift measurements and ref. 14f upper limit (time dependent Stokes shift method.) The solvation time ranges at higher temperatures are estimates which result from extrapolation of the solvation rates at lower temperatures, using an Arrhenius analysis. See ref. 12 for further details.

[b] The Sumi/Marcus and Jortner/Bixon rate predictions were made using the parameters in ref. 8, where a direct comparison was possible, and by interpolation or extrapolation where necessary. See eqns. 1–3 and refs. 7 and 12 for further details.

[c] The error in the Sumi/Marcus prediction is especially large due to the difficulty in accurately extrapolating values for the parameters required.

FIGURE CAPTIONS

Figure 1. Classical surfaces representing the charge separated ground electronic state (lower, right parabola) and the optically accessed excited electronic state (upper, left parabola) of a betaine compound. The parameters used to draw the curves come from Kjaer and Ulstrup's study[8] of betaine–26, see text. Following excitation, the reverse electron transfer occurs from the upper state back to the lower state following excitation. In theories which treat all nuclear modes classically, the electron transfer occurs in region *a*. Theories which include quantum vibrations of the solute allow electron transfer at many regions *b*, thus reducing the effective activation energy of the reverse electron transfer.

Figure 2. Reverse electron transfer dynamics of betaine–30 in (*left*) a) triacetin at 293K, b) toluene at 293K, and c) toluene at 248K, and (*right*) polystyrene at d) 293K, e) 63K, and f) 34K, exhibiting very little temperature dependence. The ordinate is the change in optical density ($-\Delta$OD, or upwards is a bleach), and the abscissa is time (picoseconds). The transients are the result of pump–probe spectroscopy at 792nm (data in panels a and b collected using the CVL amplified dye laser system) and 820nm (data in panels c through f collected using the regeneratively amplified dye laser system).

Figure 3. Arrhenius plot for the electron transfer kinetics of betaine–30 in triacetin. The nearly horizontal (solid) line at the top is the experimental data. The middle (dot and dashed) line is the prediction of Jortner/Bixon theory, which includes quantum nuclear modes of the solute. The lower (dashed) line is the Sumi/Marcus prediction, which treats all nuclear degrees of freedom classically. See text and Tables 1 and 3 for further details.

Figure 4. Arrhenius plot of the electron transfer rate of betaine–30 in polystyrene. The upper line portrays the temperature dependence of the electron transfer rate of the betaine–30 in polystyrene cast from methylene chloride solution and the lower line portrays the temperature dependent kinetics of betaine–30 in polystyrene cast from benzonitrile solution. The difference between the two lines may reflect residual solvent in the benzonitrile prepared sample.

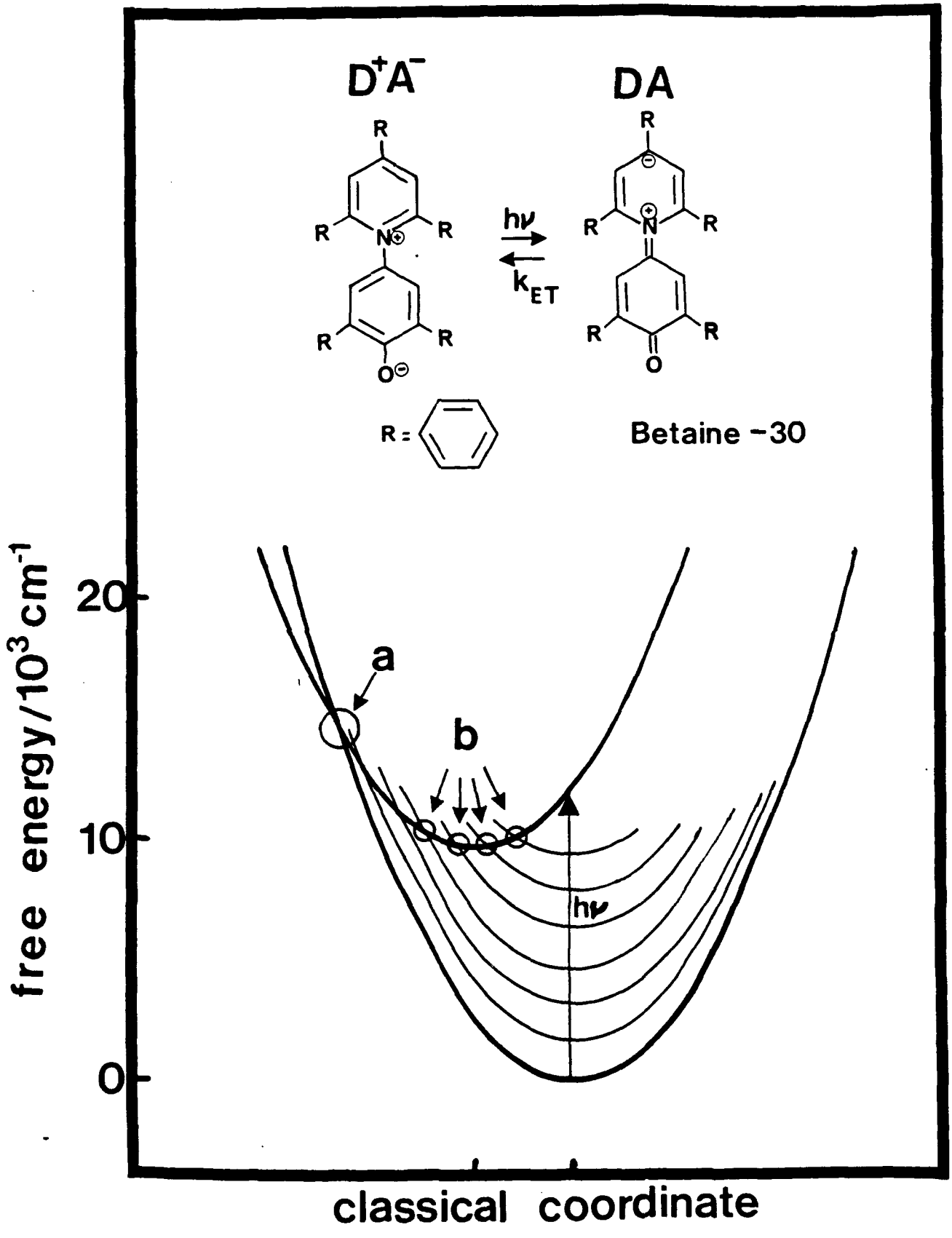
D+A−
DA
hν
k_ET
R =
Betaine −30
free energy/10³ cm⁻¹
20
10
0
a
b
hν
classical coordinate

Fig. 1

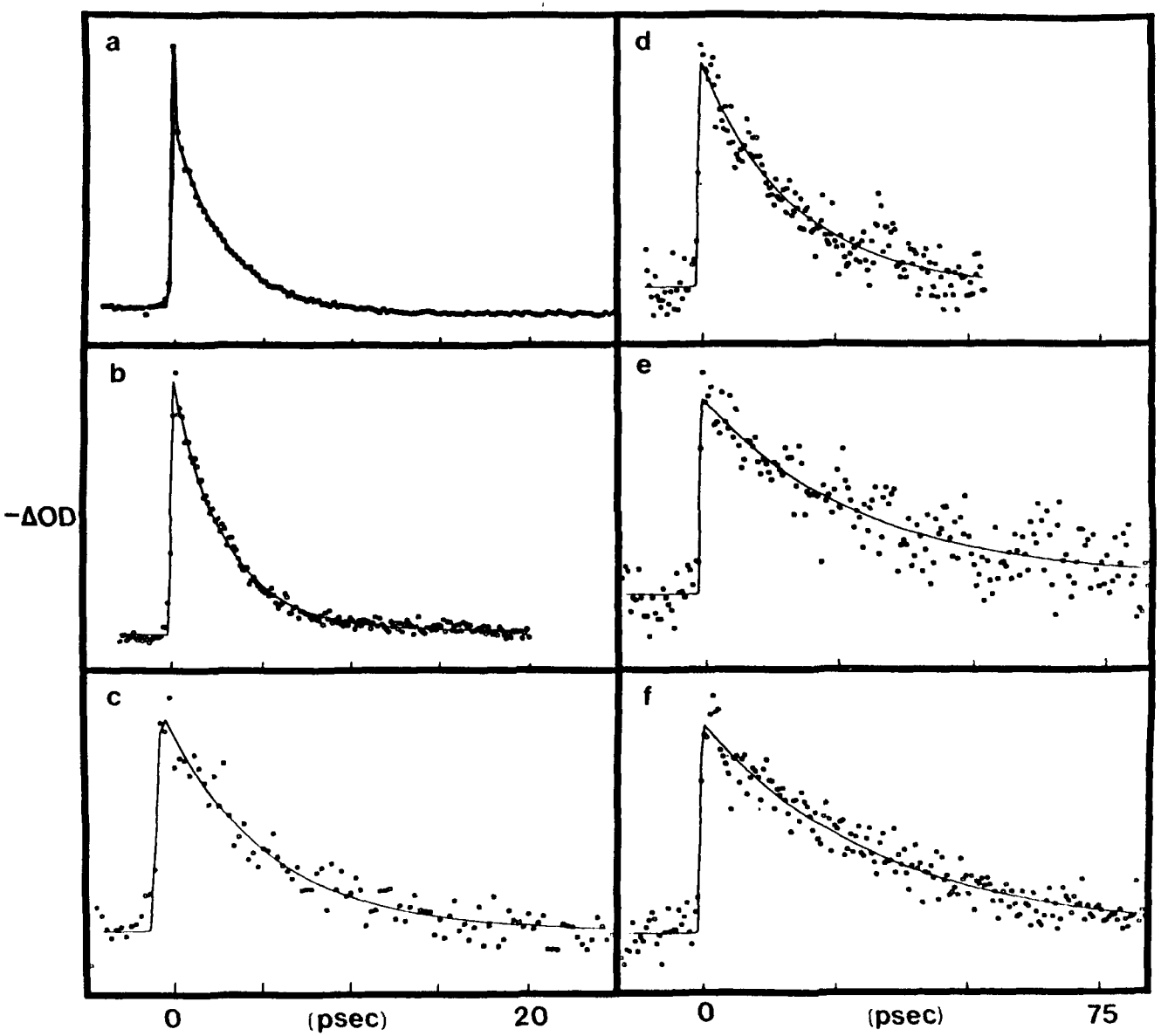

Fig. 2

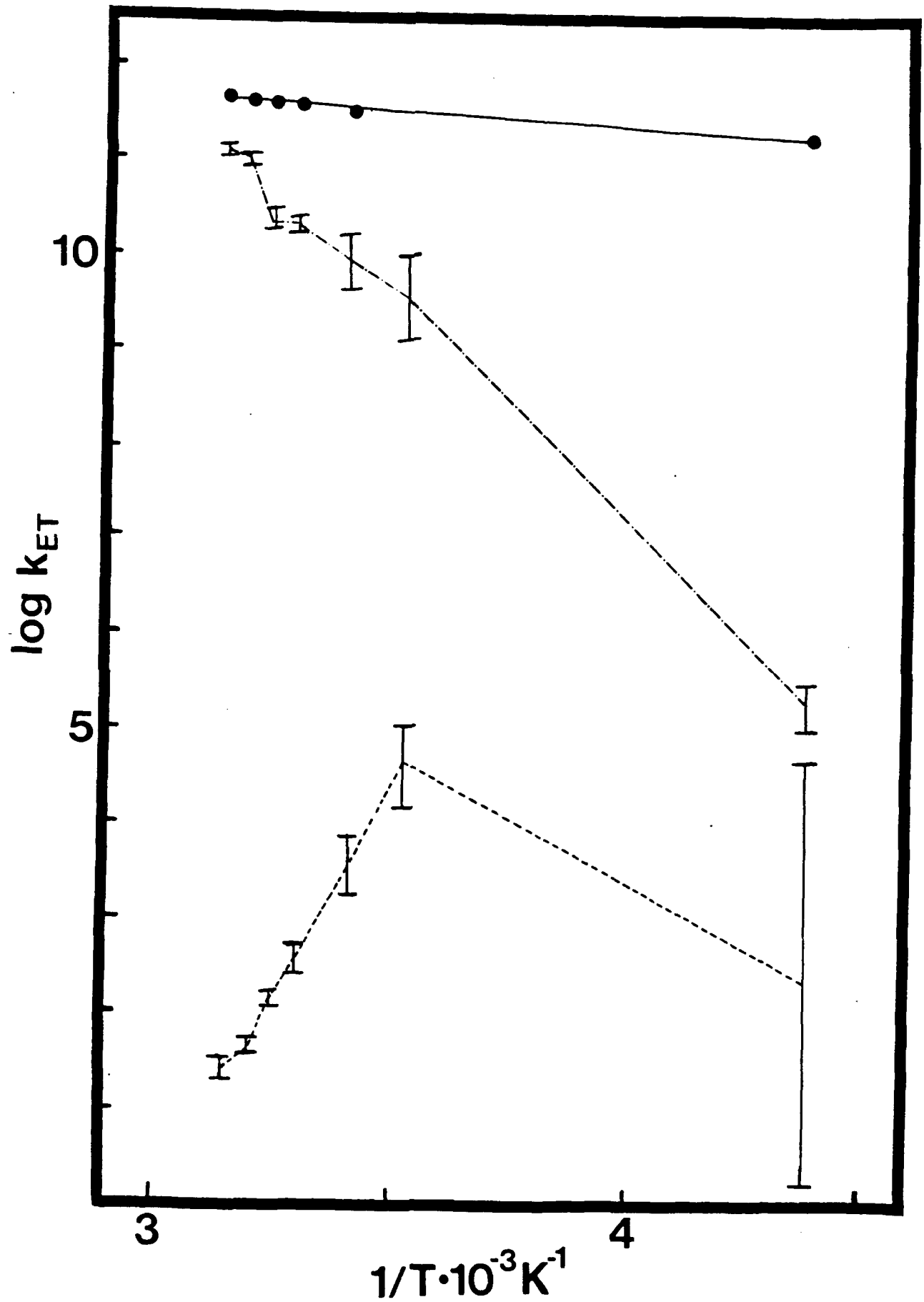

Fig. 3

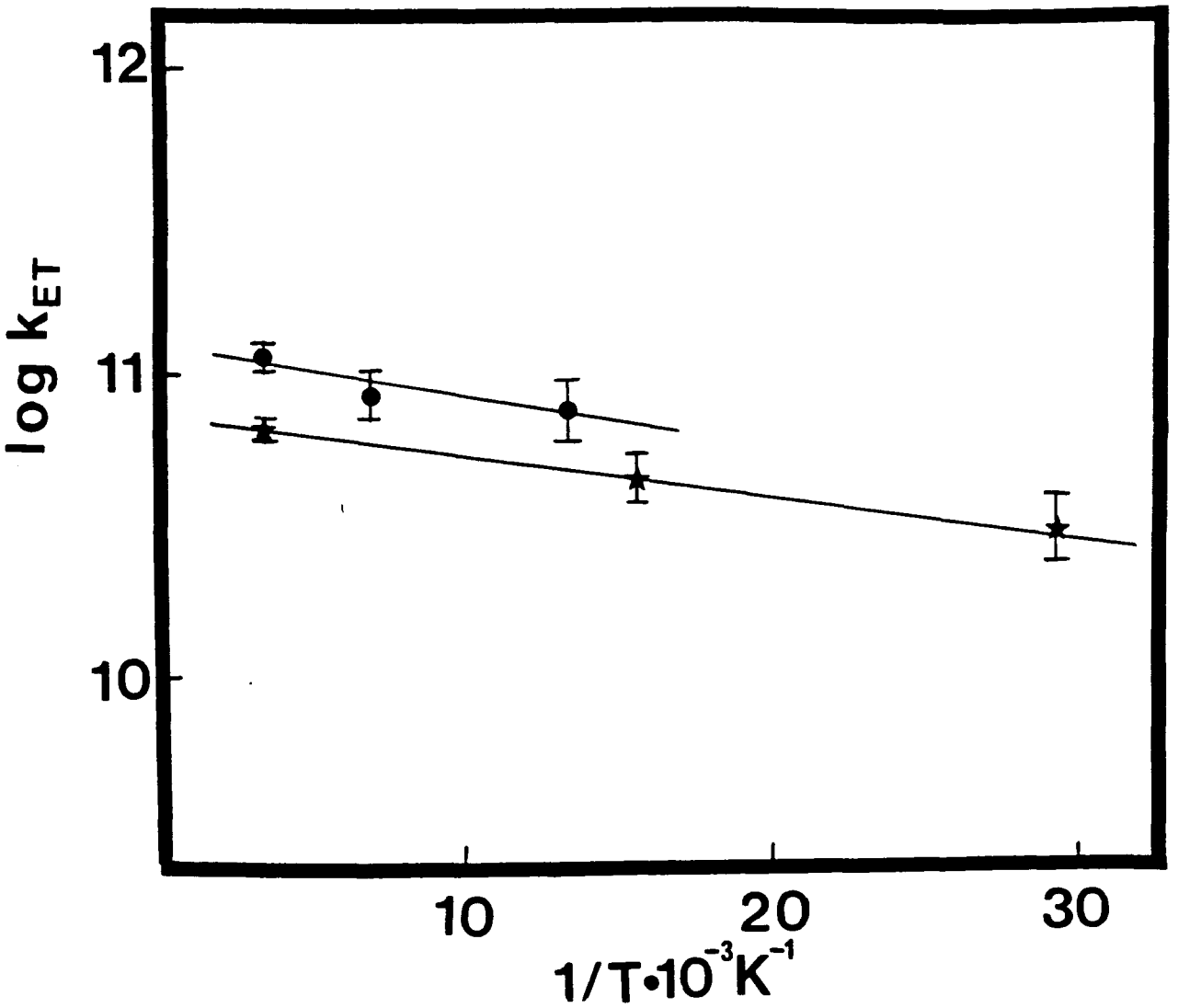

Fig. 4